

# Theoretical Study on the Relationship between Spin Multiplicity Effects and Nonlinear Optical Properties of the Pyrrole Radical (C<sub>4</sub>H<sub>4</sub>N•)

Yong-Qing Qiu,\* Hong-Ling Fan, Shi-Ling Sun, Chun-Guang Liu, and Zhong-Min Su

Institute of Functional Material Chemistry, Faculty of Chemistry, Northeast Normal University, Changchun 130024, People's Republic of China

Received: May 21, 2007; In Final Form: October 2, 2007

The geometrical structure and stability of neutral  $\pi$ -conjugated C<sub>4</sub>H<sub>4</sub>N• with three spin states were investigated by using ab initio and density functional theory (DFT) methods. In addition, the linear and nonlinear optical properties were studied at the same level combined with the finite field approach. The calculated results show that conjugation and stability decreased with increasing spin multiplicity. These reliable UCCSD results show that the polarizability ( $\alpha$ ) values of C<sub>4</sub>H<sub>4</sub>N• with the quartet state are maximal, while those of C<sub>4</sub>H<sub>4</sub>N• with the doublet state are minimal. The order of  $\beta_{\text{tot}}$  values is  $\beta_{\text{sextet}} > \beta_{\text{doublet}} > \beta_{\text{quartet}}$ . The second hyperpolarizability ( $\gamma$ ) values exhibit positive values. The variation trends of  $\gamma$  are consistent with  $\alpha$ .

## 1. Introduction

With the development of the quantum chemical theory and computer technology, it is possible to calculate the properties of molecules by using accurate theory methods. Quantum chemical calculations can be very helpful to experimental chemists who synthesize and test nonlinear optical (NLO) materials in the establishment of structure–property relationships as well as in the elucidation of mechanisms involved in the generation of NLO activity. So far, the polarizability and hyperpolarizabilities can be directly gained adopting quantum chemical theory, and we could analyze and apprehend the relationship between the molecular structure and NLO response.<sup>1–4</sup>

The organic molecules with extended  $\pi$ -delocalization have attracted great attention in scientific and technological fields because they exhibit high NLO responses, as well as their large susceptibilities, fast response, high laser damage thresholds, facility of modification, and so on.<sup>5–8</sup> During the last three decades, considerable attention has been given to the investigations of NLO properties of closed-shell systems, both experimentally and theoretically.<sup>9,10</sup> However, much less has been reported for open-shell systems. Recently, the organic radical systems are of considerable interest, which are predicted to be a promising class of new NLO materials.<sup>11–17</sup> Nakano et al. reported the spin multiplicity, basis set, and electron correlation effects on the dependency of the NLO coefficients for a series of organic radical systems. Therefore, it is possible that the highly efficient NLO materials can be obtained by modifying the spin multiplicity for open-shell systems. In order to indicate the spin multiplicity effects on the NLO coefficients, the static polarizability and hyperpolarizabilities of neutral C<sub>4</sub>H<sub>4</sub>N• with the doublet, quartet, and sextet states are studied by using ab initio and DFT methods. The present work is hoped to be a guide for the design and synthesis of open-shell NLO systems.

## 2. Modeling and Methods

Theoretically, according to an excess of  $\alpha$ -electrons with respect to  $\beta$ -electrons, there are three spin states for C<sub>4</sub>H<sub>4</sub>N•,

namely, the doublet, quartet, and sextet states. By using ab initio and DFT methods, the geometrical structures with different spin states were optimized at the 6-311g\* basis set. The C<sub>4</sub>H<sub>4</sub>N• belongs to the C<sub>2v</sub> point group. Figure 1 shows the geometrical structure and the coordinates of C<sub>4</sub>H<sub>4</sub>N•. The polarizability ( $\alpha$ ) and hyperpolarizabilities ( $\beta$ ,  $\gamma$ ) have been obtained at the 6-311g\* level by adopting the finite field (FF) approach.<sup>18</sup> Calculations have been carried out at the Hartree–Fock (HF) level as well as electron correlated methods such as the Møller–Plesset *n*th-order perturbation theory schemes (UMPn), the coupled cluster (CC) method including the single and double excitation operators (UCCSD) method. In addition, the density functional theory (DFT), that is, UB3LYP, UBHandHLYP, UB3PW91, UBPW91, and UBLYP, have also been applied. Meanwhile, an external electric field was added into the molecule containing coordinates along *x*-, *y*-, and *z*-directions. The field amplitudes are 0.0025, 0.0050, and 0.0075 au, while the field amplitudes in UMP2 and UCCSD calculations are 0.0015, 0.0030, and 0.0045 au in order to calculate well-converged values. All calculations have been performed with the Gaussian 03 program package.<sup>19</sup>

The finite field (FF) approach is used widely in calculating the molecular NLO coefficients.<sup>20–22</sup> With the static electric field, these tensor components can be described in a Taylor's expansion of the energy, as shown in eq 1:<sup>23</sup>

$$E = E^{(0)} - \mu_i F_i - \alpha_{ij} F_i F_j - \beta_{ijk} F_i F_j F_k - \gamma_{ijkl} F_i F_j F_k F_l - \dots \quad (1)$$

where  $E^{(0)}$  is the molecular energy in the absence of the applied electric field,  $F_i$  is the *i*th Cartesian component of the applied electric field, where the subscripts *i*, *j*, *k*, and *l* designate different components *x*, *y*, or *z*,  $\mu_i$  is the molecular permanent dipole moment along the *i*th direction,  $\alpha$ ,  $\beta$ , and  $\gamma$  are the linear, first, and second hyperpolarizability tensors, respectively.  $\vec{\mu}$  is the molecular total dipole moment. The  $-\vec{\mu} \cdot \vec{F}$  term represents the interaction between the external electric field and the molecule, which is added to the total Hamiltonian. A set of equations is given through calculating the system energy with each electric field, then the values of  $\mu_i$ ,  $\alpha_{ij}$ ,  $\beta_{ijk}$ , and  $\gamma_{ijkl}$  are obtained through simultaneous equations. Using the following formulas in eqs

\* Corresponding author. E-mail: qiuqy466@nenu.edu.cn.

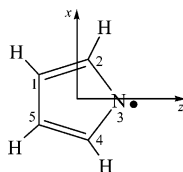


**Figure 1.** Geometrical structure and the coordinates of  $C_4H_4N\cdot$ .

**TABLE 1: Bond Length ( $\text{\AA}$ ), Dipole Moment  $\mu$  (debye), and Energy  $E$  (au) of  $C_4H_4N\cdot$  Obtained by Various Methods**

methods	multiplicity	C <sub>1</sub> –C <sub>2</sub>	C <sub>2</sub> –N <sub>3</sub>	C <sub>1</sub> –C <sub>5</sub>	$\mu_{tot}$	E
UHF	doublet	1.362	1.374	1.504	2.4495	–208.222
	quartet	1.455	1.487	1.338	2.3748	–208.091
	sextet	1.530	1.397	1.536	0.3099	–207.947
UCCSD	doublet	1.367	1.393	1.500	2.051	–208.914
	quartet	1.450	1.501	1.376	2.339	–208.761
	sextet	1.537	1.407	1.543	0.326	–208.580
UMP2	doublet	1.343	1.392	1.471	2.3663	–208.859
	quartet	1.439	1.495	1.383	2.7393	–208.709
	sextet	1.528	1.404	1.536	0.0422	–208.521
UMP3	doublet	1.346	1.395	1.484	2.3488	–208.892
	quartet	1.448	1.502	1.372	2.5908	–208.748
	sextet	1.534	1.406	1.542	0.1268	–208.567
UMP4SDQ	doublet	1.352	1.395	1.488	2.3511	–208.905
	quartet	1.449	1.503	1.375	2.5852	–208.757
	sextet	1.535	1.407	1.543	0.1543	–208.576
UB3LYP	doublet	1.363	1.385	1.495	2.3089	–209.536
	quartet	1.442	1.494	1.379	2.8241	–209.384
	sextet	1.534	1.407	1.538	0.1169	–209.202
UB3PW91	doublet	1.363	1.380	1.491	2.3325	–209.451
	quartet	1.440	1.488	1.377	2.7952	–209.299
	sextet	1.529	1.401	1.534	0.1390	–209.121
UBHandH	doublet	1.352	1.375	1.486	2.3717	–209.405
	quartet	1.437	1.482	1.358	2.7385	–209.256
	sextet	1.524	1.397	1.530	0.1457	–209.081
UBPW91	doublet	1.372	1.391	1.500	2.2738	–209.510
	quartet	1.446	1.500	1.392	2.8036	–209.359
	sextet	1.539	1.410	1.541	0.1507	–209.178
UBLYP	doublet	1.374	1.398	1.506	2.2413	–209.456
	quartet	1.451	1.510	1.397	2.8142	–209.305
	sextet	1.362	1.374	1.504	0.1262	–209.121

2–4, the polarizability ( $\alpha$ ) and hyperpolarizabilities ( $\beta_{tot}, \gamma$ ) are obtained:

$$\alpha = (\alpha_{xx} + \alpha_{yy} + \alpha_{zz})/3 \quad (2)$$

$$\beta_{tot} = (\beta_x^2 + \beta_y^2 + \beta_z^2)^{1/2} \quad (3)$$

where  $\beta_i$  is

$$\beta_i = \beta_{iii} + \sum_{i \neq j} [(\beta_{ijj} + 2\beta_{jji})/3] \quad i = x, y, z$$

$$\gamma = 1/5 \{ \gamma_{xxxx} + \gamma_{yyyy} + \gamma_{zzzz} + 2[\gamma_{xxyy} + \gamma_{xxzz} + \gamma_{yyzz}] \} \quad (4)$$

### 3. Results and Discussion

**3.1. Geometrical Structures and Stability of  $C_4H_4N\cdot$  with Different Spin States.** The bond lengths, dipole moments, and energies of  $C_4H_4N\cdot$  with different spin states obtained by various methods are listed in Table 1. With an increase of the spin multiplicity, the energy of the system increases, that is, the stability of the molecule with the high spin state is lower. For  $C_4H_4N\cdot$  with each spin state, the molecular energy obtained by ab initio methods is higher than that obtained by DFT methods. The energy obtained by the DFT/UB3LYP method is minimal.

By analyzing the variation of C–C and C–N bond lengths in Table 1 and Figure 2, it is found that similar trends are obtained by various methods (except for UBLYP). For  $C_4H_4N\cdot$  with the doublet state, the C<sub>2</sub>–N<sub>3</sub> bond length is intervariant between C–N single-bond (1.48  $\text{\AA}$ ) and double-bond values (1.28  $\text{\AA}$ ), while the C<sub>1</sub>–C<sub>2</sub> bond length is close to the C–C

**TABLE 2: Expectation Values ( $\langle S^2 \rangle$ ) of  $C_4H_4N\cdot$  with the Doublet, Quartet, and Sextet States**

methods	doublet	quartet	sextet
UHF	1.092	3.780	8.804
UCCSD	1.101	3.781	8.806
UMP2	1.036	3.780	8.806
UMP3	1.049	3.781	8.806
UMP4SDQ	1.064	3.781	8.806
UB3LYP	0.779	3.759	8.766
UB3PW91	0.783	3.759	8.767
UBHandH	0.820	3.764	8.775
UBPW91	0.767	3.757	8.763
UBLYP	0.764	3.757	8.760
Exact	0.750	3.750	8.750

double-bond value (1.34  $\text{\AA}$ ), and the C<sub>1</sub>–C<sub>5</sub> bond length is close to the C–C single-bond value (1.54  $\text{\AA}$ ). So the five atoms in the molecular framework formed a conjugated bond  $\pi_5^5$  along the C<sub>1</sub>–C<sub>2</sub>–N<sub>3</sub>–C<sub>4</sub>–C<sub>5</sub> direction. The conjugated structure of neutral  $C_4H_4N\cdot$  is different from that of  $C_4H_4NH$ . On the other hand, for  $C_4H_4N\cdot$  with the quartet state, the C<sub>1</sub>–C<sub>2</sub> bond length is intervariant between those of a single bond and a double bond, while the C<sub>2</sub>–N<sub>3</sub> bond length is close to the single-bond value, and the C<sub>1</sub>–C<sub>5</sub> shows obvious double-bond character. The conjugated bond  $\pi_4^4$  is formed by four atoms in the framework along the C<sub>2</sub>–C<sub>1</sub>–C<sub>5</sub>–C<sub>4</sub> direction. It is clearly seen that the number of conjugated atoms in  $C_4H_4N\cdot$  with the quartet state is less than that in the doublet state. For  $C_4H_4N\cdot$  with the sextet state, all bond lengths are close to single bonds, thus conjugated  $\pi$ -bonds disappear. Therefore, the conjugation and stability of  $C_4H_4N\cdot$  are shown to decrease when the spin multiplicity changed from the doublet to the sextet state. The reason is that  $\pi$ -bonds are broken by increasing the spin multiplicity. This feature is in good agreement with the variation of molecular energy.

Meanwhile, the dipole moments of  $C_4H_4N\cdot$  with three spin states are listed in Table 1. The results show that the trend of the dipole moments at UMPn, UCCSD, and DFT levels is uniform, that is,  $\mu_{quartet} > \mu_{doublet} > \mu_{sextet}$ . Moreover, the difference between the doublet and the quartet states is larger than that between the quartet and the sextet states. The dipole moment of  $C_4H_4N\cdot$  with the sextet state is tiny, so the  $C_4H_4N\cdot$  with the sextet state is closed to a nonpolar molecule. It indicates that five  $\pi$ -electrons localized on each atom and the delocalized covalent bonds do not exist. The feature corresponds to the geometrical structure of  $C_4H_4N\cdot$ .

**3.2. Spin Contaminations.** For open-shell systems, the unrestricted self-consistent-field (SCF) orbitals are selected as the origin of the single configuration-based many-body perturbation (MBP) or couple cluster (CC) theory. Because the unrestricted SCF wave function is no longer an eigenfunction of the total spin,  $\langle S^2 \rangle$ , some error called spin contamination may be introduced into the calculation. The expectation value of  $\langle S^2 \rangle$  obtained by ab initio and DFT levels of approximations are listed in Table 2. It is clearly seen that the  $\langle S^2 \rangle$  values are much larger in UHF, UCCSD, and UMPn calculations than that in DFT calculations. At the ab initio level, the  $\langle S^2 \rangle$  values of the  $C_4H_4N\cdot$  with the doublet state are larger than 1.00 and indicate that spin contaminations are more than one-third of the exact value, while those of the  $C_4H_4N\cdot$  with the quartet and sextet states are similar to the exact ones. It suggests that the spin contamination is negligible for  $C_4H_4N\cdot$  with the high spin state. In general, spin contamination is negligible when the spin multiplicity is larger than three.<sup>24</sup> In addition, it is less evident to find any significant spin contamination in DFT calculations, so it is selected to calculate the open-shell systems. In order to minimize the errors

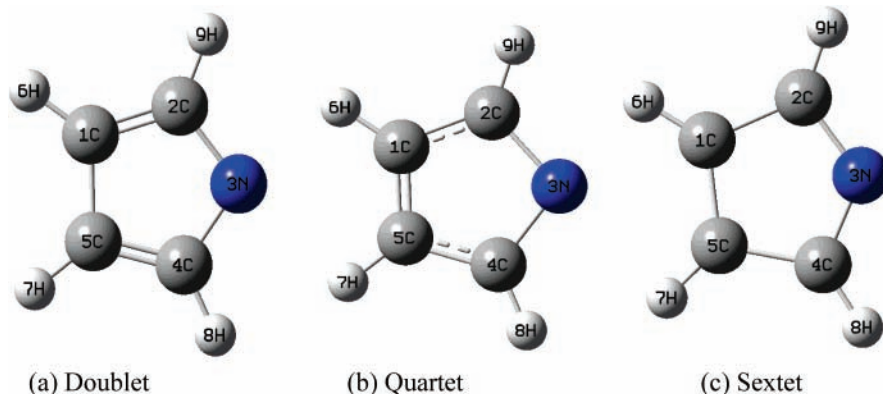


**Figure 2.** Geometrical structure of C<sub>4</sub>H<sub>4</sub>N• optimized by the UB3LYP method.

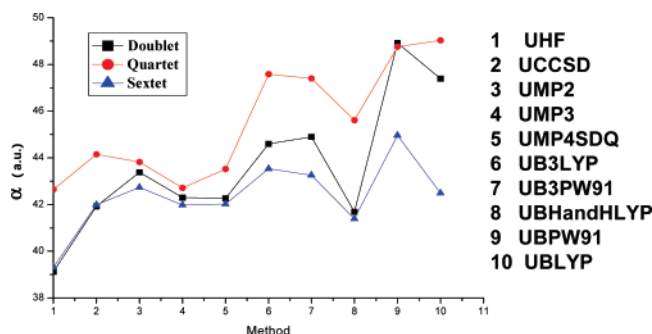


**Figure 3.** The  $\alpha$  values of C<sub>4</sub>H<sub>4</sub>N• with the doublet, quartet, and sextet states obtained by various methods.

caused by the spin contamination, spin-projected methods, such as PUMPn and PUHF, have been applied. The technique of self-annihilation in calculation methods is a better method to correct spin contamination.

**3.3. Linear and Nonlinear Optical Coefficients.** 3.3.1. *Polarizability ( $\alpha$ ).* Figure 3 shows the  $\alpha$  values of C<sub>4</sub>H<sub>4</sub>N• with different spin multiplicity obtained by different methods. For C<sub>4</sub>H<sub>4</sub>N• with each spin state, the  $\alpha$  values obtained by ab initio methods are smaller than those obtained by DFT methods (except for UBHandHLYP and UBLYP). For C<sub>4</sub>H<sub>4</sub>N• with the doublet and sextet states, the UBHandHLYP, UBLYP, UMP2, UMP3, and UMP4SDQ values give similar  $\alpha$  values compared with the UCCSD values. For C<sub>4</sub>H<sub>4</sub>N• with the quartet state, the DFT methods give larger  $\alpha$  values compared with the UCCSD method, whereas the UHF and UMPn methods give smaller  $\alpha$  values. The UMP2 and UBHandHLYP values are very close to the UCCSD value. In addition, the order of  $\alpha$  values obtained by the UHF method is the same as that obtained by the UCCSD method, that is,  $\alpha_{\text{quartet}} > \alpha_{\text{sextet}} > \alpha_{\text{doublet}}$ . For the UMPn and DFT methods, the  $\alpha$  values of C<sub>4</sub>H<sub>4</sub>N• with the doublet state are larger than those with the sextet state. The C<sub>4</sub>H<sub>4</sub>N• with the intermediate spin state has the largest  $\alpha$  values.

3.3.2. *First Hyperpolarizability ( $\beta_{\text{tot}}$ ).* The C<sub>4</sub>H<sub>4</sub>N• belongs to C<sub>2v</sub> symmetry, so several  $\beta$  tensor values are zero. Combining other tensors with the formula in eq 3, we obtained the total second hyperpolarizability ( $\beta_{\text{tot}}$ ). In Table 3 and Figure 4, we present the components of  $\beta$  and the  $\beta_{\text{tot}}$  values of C<sub>4</sub>H<sub>4</sub>N• with different spin state. The calculated results show  $\beta_{xxz}$  and  $\beta_{zzz}$  are the dominant contributors to the second-order nonlinear response. For C<sub>4</sub>H<sub>4</sub>N• with the doublet state, the  $\beta_{\text{tot}}$  values obtained by UMPn methods overestimate the  $\beta_{\text{tot}}$  value compared with that by the most reliable UCCSD method, while the DFT methods, especially the UBHandHLYP method, give similar  $\beta_{\text{tot}}$  values. The UHF method gives a very small value compared with the UCCSD method. For C<sub>4</sub>H<sub>4</sub>N• with the

quartet, the  $\beta_{\text{tot}}$  values obtained by UMPn methods are much larger than that obtained by the UCCSD method, whereas the  $\beta_{\text{tot}}$  values obtained by UHF, UB3LYP, UB3PW91, and UBHandHLYP methods are similar to that obtained by the UCCSD method. For C<sub>4</sub>H<sub>4</sub>N• with the sextet state, the UHF and DFT values are smaller than the UCCSD values, whereas the UMPn values are overestimated. In addition, the  $\beta_{\text{tot}}$  values obtained by UHF and UBHandHLYP methods are very close to those obtained by the UCCSD method.

On the other hand, the spin multiplicity effects on  $\beta_{\text{tot}}$  are investigated by comparing three spin states of the C<sub>4</sub>H<sub>4</sub>N•. For the low and high spin states, all methods except for UBLYP and UBPW91 show that the order of  $\beta_{\text{tot}}$  with the doublet and sextet states is  $\beta_{\text{sextet}} > \beta_{\text{doublet}}$ . For the intermediate spin (the quartet state) the  $\beta_{\text{tot}}$  values obtained by UMPn methods are larger than those with the sextet. The  $\beta_{\text{tot}}$  values obtained by UB3LYP, UB3PW91, and UBHandHLYP methods are smaller than those with the doublet, which is consistent with those obtained by the UCCSD and UCCSD(T) methods. Again, the UHF method cannot predict the tendency of  $\beta_{\text{tot}}$ .

The first hyperpolarizability is related to the electron transition and the conjugated structure. The unpaired electrons of C<sub>4</sub>H<sub>4</sub>N• increased when the spin multiplicity changed from the doublet to the sextet state. The possibility of electron transition was enhanced and the  $\beta_{\text{tot}}$  value is larger. In addition, the conjugation with the quartet state is smaller than that with the doublet state. So the C<sub>4</sub>H<sub>4</sub>N• with the quartet state exhibited the smaller  $\beta_{\text{tot}}$  value.

3.3.3. *Second Hyperpolarizability ( $\gamma$ ).* The second hyperpolarizability ( $\gamma$ ) is the fourth-order tensor, which is much more complicated than  $\beta$ . The average  $\gamma$  value was calculated by combining the  $\beta$  values with the formula in eq 4. The results of C<sub>4</sub>H<sub>4</sub>N• with the doublet, quartet, and sextet states obtained by various methods are listed in Table 4. We confine our attention to the longitudinal component of static  $\gamma$  ( $\gamma_{zzzz}$ ), which dominates the response in  $\pi$ -conjugated systems. The order of  $\gamma_{zzzz}$  obtained by the UCCSD method is  $\gamma_{\text{quartet}} > \gamma_{\text{sextet}} > \gamma_{\text{doublet}}$ , which is the same as the order of  $\gamma$ . For C<sub>4</sub>H<sub>4</sub>N• with the doublet state, except that the UBPW91 and UBLYP methods give negative  $\gamma$  values, other methods give positive  $\gamma$  values. Moreover, the  $\gamma$  values obtained by the UMPn, UBHandHLYP, and UHF methods are smaller than that obtained by the reliable UCCSD method. The UB3LYP value is very close to the UCCSD value, whereas the UB3PW91 value is overestimated. For C<sub>4</sub>H<sub>4</sub>N• with the quartet state, the UMPn methods give negative  $\gamma$  values and overshoot the  $\gamma$  values compared with the UCCSD value, which is positive in sign. The DFT methods provide a positive  $\gamma$  and these values are underestimated. The UHF method reproduces closer  $\gamma$  values compared with the UCCSD method.

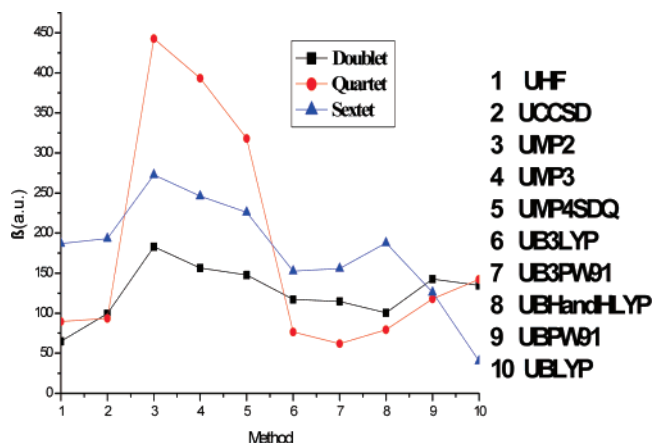


**TABLE 3: Components of  $\beta$  and  $\beta_{\text{tot}}$  Values of  $\text{C}_4\text{H}_4\text{N}^\bullet$  with the Doublet, Quartet, and Sextet States Obtained by Various Methods (au)**

methods	multiplicity	$\beta_{zzz}$	$\beta_{xxz}$	$\beta_{yyz}$	$\beta_{\text{tot}}$
UHF	doublet	-68.603	50.212	-10.684	65.142
	quartet	104.491	-76.965	-18.927	89.733
	sextet	-146.780	-99.719	16.742	187.011
UCCSD	doublet	-91.417	121.267	-17.178	99.386
	quartet	80.954	29.351	-18.571	93.646
	sextet	-168.028	-67.419	7.500	193.364
UCCSD(T)	doublet	-41.870	120.862	-10.267	81.020
	quartet	60.212	18.446	-2.616	66.656
	sextet	-75.096	-34.872	-1.815	90.375
UMP2	doublet	-190.548	74.839	-28.623	183.107
	quartet	210.424	419.503	-22.273	442.685
	sextet	-229.548	-101.536	-2.342	272.713
UMP3	doublet	-163.773	65.362	-22.713	156.510
	quartet	161.394	400.644	-18.976	393.446
	sextet	-203.266	-103.080	3.098	246.380
UMP4SDQ	doublet	-155.532	66.167	-20.938	147.880
	quartet	141.618	313.307	-19.274	318.142
	sextet	-189.229	-88.831	2.408	225.942
UB3LYP	doublet	-115.461	119.550	-25.722	117.189
	quartet	-2.159	-94.594	-21.604	76.528
	sextet	-145.934	-21.721	4.241	152.476
UB3PW91	doublet	-114.704	107.914	-26.712	114.774
	quartet	22.366	-88.143	-21.899	62.218
	sextet	-146.783	-27.598	4.247	155.684
UBHandHLYP	doublet	-103.445	86.101	-19.851	100.447
	quartet	96.271	-58.953	-58.953	79.591
	sextet	-166.709	-57.466	6.602	187.668
UBPW91	doublet	-131.252	8.138	-36.287	142.804
	quartet	-51.164	-106.550	-20.187	118.120
	sextet	-126.780	-0.588	3.193	125.930
UBLYP	doublet	-136.541	105.227	-33.639	134.613
	quartet	-78.205	-109.896	-19.520	142.342
	sextet	-43.690	11.738	0.347	40.427

For  $\text{C}_4\text{H}_4\text{N}^\bullet$  with the sextet state, all methods give positive  $\gamma$  values. The UHF, UBLYP, and UMPn values are similar to the UCCSD value, whereas the DFT (except for UBLYP) values are underestimated. The positive  $\gamma$  value causes the self-focusing effect of an incident beam, while the negative one does self-defocusing effect.<sup>25,26</sup> Therefore, it is possible that the  $\text{C}_4\text{H}_4\text{N}^\bullet$  has the character of self-focusing behavior. Furthermore, the spin multiplicity effects influence the  $\gamma$  values of  $\text{C}_4\text{H}_4\text{N}^\bullet$ . The magnitude of  $\gamma$  values with intermediate spin state by the UMPn and UCCSD methods is larger than that with the doublet and the sextet states, that is,  $\gamma_{\text{quartet}} > \gamma_{\text{sextet}} > \gamma_{\text{doublet}}$ . The UBHandHLYP, UHF and UMPn methods provide the same trend as the UCCSD method.

The variations in  $\gamma$  value with three spin states are related to the electron correlation regime. In general, open-shell systems can be classified according to the strength of electron correlation,

**Figure 4.** The  $\beta_{\text{tot}}$  values of  $\text{C}_4\text{H}_4\text{N}^\bullet$  with the doublet, quartet, and sextet states obtained by various methods.

i.e., weak-, intermediate-, and strong (magnetic)-correlation regimes. The studies have suggested the enhancement of  $\gamma$  in the intermediate correlation regime. For  $\text{C}_4\text{H}_4\text{N}^\bullet$ , the intermediate correlation regime (the quartet state) is associated with the largest  $\gamma$  value. However, for the weak and strong correlation regimes, the  $\gamma$  values are smaller. The feature is understood by the fact that the intermediate bonding electrons are sensitive to the applied field, leading to large fluctuation.

**3.4. Basis Set Effects on the Polarizability and the Hyperpolarizabilities.** In general, the basis set dependences of hyperpolarizabilities are important for open-shell systems with intermediate spin state. So, the static  $\alpha$ ,  $\beta_{\text{tot}}$ , and  $\gamma$  values of the  $\text{C}_4\text{H}_4\text{N}^\bullet$  with the quartet states were calculated with the UMP2 and UB3LYP methods by using different basis sets. The results are listed in Table 5, which show that all basis sets provide similar  $\alpha$  values. The 6-31g\* basis set underestimates  $\alpha$  values compared to the addition of diffuse functions, the 6-31+g\* basis set, while the 6-31+g\*\* basis set provides similar  $\alpha$  values. This shows it is not necessary to add a polarizability function on H atoms. Meanwhile, the 6-311g\* basis set also provides larger  $\alpha$  values compared to the 6-31g\* basis set. For the UB3LYP method, the 6-31+g\* and the 6-31+g\*\* basis sets provide the closer  $\beta_{\text{tot}}$  values, which are smaller than that at the 6-31g\* basis set. The  $\beta_{\text{tot}}$  value at the 6-311g\* basis set is larger than that at the 6-31+g\* and 6-31+g\*\* basis sets. So, the diffuse functions lead to decreased  $\beta_{\text{tot}}$ . For the UMP2 method, the 6-311g\* basis set gives larger  $\beta_{\text{tot}}$  values compared with the 6-31g\* basis set, that is, the  $\beta_{\text{tot}}$  values increase with enhancing basis functions. The  $\beta_{\text{tot}}$  values obtained with the 6-31+g\* and 6-31+g\*\* basis sets are larger than that obtained with the 6-31g\* basis set. In addition, at the UB3LYP level, the 6-31+g\* and 6-31+g\*\* basis sets provide similar  $\gamma$  values compared to the 6-31g\* and 6-311g\* basis sets. At the UMP2

**TABLE 4: Components of  $\gamma$  (au) and  $\gamma$  Values of C<sub>4</sub>H<sub>4</sub>N• with the Doublet, Quartet, and Sextet States Obtained by Various Methods**

methods	multiplicity	$\gamma_{xxxx}$	$\gamma_{yyyy}$	$\gamma_{zzzz}$	$\gamma_{xyyy}$	$\gamma_{xxzz}$	$\gamma_{yyzz}$	$\gamma$
UHF	doublet	3798	209	3223	182	1803	621	2489
	quartet	-18303	-100	10190	539	19478	382	6517
	sextet	7674	-12	7792	274	3616	488	4842
UCCS D	doublet	7339	4304	1171	1763	2529	518	4487
	quartet	-13188	-134	8391	10143	6469	921	6027
	sextet	5366	145	8262	2187	3523	190	5115
UMP2	doublet	6191	96	1054	218	2144	1356	2955
	quartet	-199057	-43	14399	672	-3738	519	-37959
	sextet	3809	463	12371	1010	3172	222	5091
UMP3	doublet	5525	62	1212	159	2068	1098	2690
	quartet	-177319	-181	12554	885	9840	114	-28653
	sextet	4963	329	11054	862	3338	287	5064
UMP4 SDQ	doublet	5593	-198	1645	131	219	1007	2707
	quartet	-97098	599	11557	-2361	4242	872	-15887
	sextet	4485	302	10157	898	3137	263	4708
UB3L YP	doublet	17675	101	2311	-725	-587	1607	4136
	quartet	-2890	45	3786	988	5335	892	3074
	sextet	3205	218	6639	1095	2648	581	3742
UB3P W91	doublet	30085	120	2136	-1239	-1797	1742	5950
	quartet	-2561	57	3752	899	5383	835	3097
	sextet	3194	230	7254	986	2691	502	3807
UBHa ndH	doublet	9624	158	1607	-20	1533	1101	3324
	quartet	-807	19	5854	773	5764	734	3921
	sextet	3699	206	7899	793	2536	472	3881
UBPW 91	doublet	-225190	-22	3372	-3892	-8979	2809	-48392
	quartet	-4201	74	4372	1073	5144	889	2892
	sextet	3417	229	6205	1226	3028	604	3913
UBLY P	doublet	-48526	-36	3851	-1292	-3660	2426	-9953
	quartet	-4094	525	5225	1208	5099	942	3137
	sextet	4952	208	4930	2820	3166	2359	5356

**TABLE 5: Basis-Set Effects on  $\alpha$ ,  $\beta_{\text{tot}}$ , and  $\gamma$  of C<sub>4</sub>H<sub>4</sub>N• with the Quartet State (au)**

methods/basis sets	$\alpha$	$\beta_{\text{tot}}$	$\gamma$
UB3LYP/6-31g*	42.458	144.639	3163.776
UB3LYP/6-31+g*	57.219	50.183	51705.867
UB3LYP/6-31+g**	57.641	50.942	51841.350
UB3LYP/6-311g*	47.578	76.528	3074.103
UMP2/6-31g*	40.884	359.319	-17293.700
UMP2/6-31+g*	52.610	619.945	-13680.775
UMP2/6-31+g**	52.374	648.814	-24123.856
UMP2/6-311g*	43.822	442.685	-37958.988

level, the  $\gamma$  value at the 6-31+g\*\* basis set is much larger than that with the 6-31+g\* and 6-31g\* basis sets. The 6-311g\* basis set provides the larger  $\gamma$  value. So, in order to reduce calculation time and enhance the reliable results, the 6-311g\* basis set was employed.

#### 4. Conclusions

Geometrical structure, stability, the basis set effects, and the linear and nonlinear optical properties were calculated for neutral C<sub>4</sub>H<sub>4</sub>N• in the doublet, quartet, and sextet states. The results indicate that conjugation and stability of the neutral C<sub>4</sub>H<sub>4</sub>N• decreased subsequently with an increase of its spin multiplicity. It is necessary that spin contamination is considered for open-shell systems. However, spin contamination effects can be ignored when the value of the spin multiplicity is larger than three.

The linear and nonlinear optical coefficients for neutral C<sub>4</sub>H<sub>4</sub>N• were calculated by using the reliable UCCSD method. The UCCSD results show that  $\alpha$ ,  $\beta_{\text{tot}}$ , and  $\gamma$  values of C<sub>4</sub>H<sub>4</sub>N• also changed with changing the spin multiplicity. The  $\alpha$  values of C<sub>4</sub>H<sub>4</sub>N• with the quartet state are maximal, while that of C<sub>4</sub>H<sub>4</sub>N• with the doublet state are minimal. The variation trend of the  $\beta_{\text{tot}}$  value is different from that of  $\alpha$ , that is, the order of  $\beta_{\text{tot}}$  values is  $\beta_{\text{sextet}} > \beta_{\text{doublet}} > \beta_{\text{quartet}}$ . In addition, the  $\gamma$  value

of C<sub>4</sub>H<sub>4</sub>N• with the intermediate spin state (the quartet state) is larger than that with the doublet and sextet states, that is,  $\gamma_{\text{quartet}} > \gamma_{\text{sextet}} > \gamma_{\text{doublet}}$ . It is obvious that the variation trend of  $\gamma$  values is in agreement with that of  $\alpha$ .

For such systems, the highly correlated method (UCCSD) turns out to be necessary for a NLO property study. Compared with the UCCSD method, the UBHandHLYP, UB3LYP, and UB3PW91 give the closer  $\beta_{\text{tot}}$  value and predict the same variation trend of  $\beta_{\text{tot}}$  for three spin states. In addition, the  $\gamma$  values obtained by the UHF and UBHandHLYP methods are a rather good approximation with that obtained by the UCCSD method.

Hence, the NLO activities can be modified by controlling the spin multiplicity. The spin-controlling schemes have been proposed in the molecular magnetic field for open-shell compounds. Therefore, it is important to consider the correlation between NLO and magnetic properties for designing and synthesizing new multifunctional materials in the exploitation of new materials.

**Acknowledgment.** This work was Supported by the Program for Changjiang Scholars and Innovative Research Team in University, the Foundation of Jilin Provincial Excellent Youth (Grant No. 20050107), and the Youth Science Foundation of Northeast Normal University (Grant No. 20060314).

#### References and Notes

- (1) Gisbergen, J. A.; Snijders, J. G.; Baerends, J. *Phys. Rev. Lett.* **1997**, *21*, 3097.
- (2) Marcus, S. L.; Chao, Y.; Dickey, J. O.; Cegout, P. *Science* **1998**, *281*, 1656.
- (3) Lan, Y. Z.; Cheng, W. D.; Wu, D. S.; Li, X. D.; Zhang, H.; Gong, Y. J. *Chem. Phys. Lett.* **2003**, *372*, 645.
- (4) Liu, C. L.; Su, Z. M.; Feng, J. K.; Ren, A. M.; Su, J. Z.; Cha, Z. Z.; Wang, Q. *Acta Chim. Sinica* **2000**, *58*, 184 (in Chinese).
- (5) Nakano, M.; Yamaguchi, K. *Chem. Phys. Lett.* **1993**, *206*, 285.

- (6) Nakano, M.; Yamaguchi, K. *Mol. Cryst. Liq. Cryst., A* **1994**, 255, 139.
- (7) Kanis, D. R.; Ratner, M. A.; Marks, T. *J. Chem. Rev.* **1994**, 94, 195.
- (8) Brédas, J. L.; Adant, C.; Tackx, P.; Persoons, A. *Chem. Rev.* **1994**, 94, 243.
- (9) Andreu, R.; Blesa, M. J.; Carrasquer, L.; Garín, J.; Orduna, J.; Villacampa, B.; Alcalá, R.; Casado, J.; Delgado, M. C. R.; Navarrete, J. T. L.; Allain, M. *J. Am. Chem. Soc.* **2005**, 127, 8835.
- (10) Bretung, E. M.; Shu, C. F.; McMahon, R. J. *J. Am. Chem. Soc.* **2000**, 122, 1154.
- (11) Nakano, M.; Nagao, H.; Yamaguchi, K. *Phys. Rev. A* **1997**, 55, 1503.
- (12) Nakano, M.; Yamada, S.; Yamaguchi, K. *Chem. Phys. Lett.* **1999**, 311, 221.
- (13) Kamada, K.; Ohta, K.; Nakamura, J.; Yamada, S.; Nakano, M.; Yamaguchi, K. *Mol. Cryst. Liq. Cryst.* **1998**, 315, 117.
- (14) Nakano, M.; Nitta, T.; Yamaguchi, K.; Champagne, B.; Botek, E. *J. Phys. Chem. A* **2004**, 108, 4105.
- (15) Champagne, B.; Botek, E.; Nakano, M.; Nitta, T.; Yamaguchi, K. *J. Chem. Phys.* **2005**, 122, 114315.
- (16) Nakano, M.; Kishi, R.; Nitta, T.; Kubo, T.; Nakasuji, K.; Kamada, K.; Ohta, K.; Champagne, B.; Botek, E.; Yamaguchi, K. *J. Phys. Chem. A* **2005**, 109, 885.
- (17) Nakano, M.; Kishi, R.; Nakagawa, N.; Ohta, S.; Takahashi, H.; Furukawa, S.; Kamada, K.; Ohta, K.; Champagne, B.; Botek, E.; Yamada, S.; Yamaguchi, K. *J. Phys. Chem. A* **2006**, 110, 4238.
- (18) Kurtz, H. A.; Stewart, J. J. P.; Dieter, K. M. *J. Comput. Chem.* **1990**, 11, 82.
- (19) Frisch, M. J.; Trucks, G. W.; Schlegel, H. B.; Scuseria, G. E.; Robb, M. A.; Cheeseman, J. R.; Montgomery, J. A., Jr.; Vreven, T.; Kudin, K. N.; Burant, J. C.; Millam, J. M.; Iyengar, S. S.; Tomasi, J.; Barone, V.; Mennucci, B.; Cossi, M.; Scalmani, G.; Rega, N.; Petersson, G. A.; Nakatsuji, H.; Hada, M.; Ehara, M.; Toyota, K.; Fukuda, R.; Hasegawa, J.; Ishida, M.; Nakajima, T.; Honda, Y.; Kitao, O.; Nakai, H.; Klene, M.; Li, X.; Knox, J. E.; Hratchian, H. P.; Cross, J. B.; Bakken, V.; Adamo, C.; Jaramillo, J.; Gomperts, R.; Stratmann, R. E.; Yazyev, O.; Austin, A. J.; Cammi, R.; Pomelli, C.; Ochterski, J. W.; Ayala, P. Y.; Morokuma, K.; Voth, G. A.; Salvador, P.; Dannenberg, J. J.; Zakrzewski, V. G.; Dapprich, S.; Daniels, A. D.; Strain, M. C.; Farkas, O.; Malick, D. K.; Rabuck, A. D.; Raghavachari, K.; Foresman, J. B.; Ortiz, J. V.; Cur, Q.; Baboul, A. G.; Clifford, S.; Cioslowski, J.; Stefanov, B. B.; Liu, G.; Liashenko, A.; Piskorz, P.; Komaromi, I.; Martin, R. L.; Fox, D. J.; Keith, T.; Al-Laham, M. A.; Peng, C. Y.; Nanayakkara, A.; Challacombe, M.; Gill, P. M. W.; Johnson, B.; Chen, W.; Wong, M. W.; Gonzalez, C.; Pople, J. A. *Gaussian 03*, revision C.02; Gaussian, Inc.: Wallingford, CT 2004.
- (20) Cohen, H. D.; Roothaan, C. C. J. *J. Chem. Phys.* **1965**, 43, S34.
- (21) Qiu, Y. Q.; Qin, C. S.; Su, Z. M.; Yang, G. C.; Pan, X. M.; Wang, R. S. *Synth. Met.* **2005**, 152, 273.
- (22) Nakano, M.; Fujita, H.; Takahata, M.; Yamaguchi, K. *J. Am. Chem. Soc.* **2002**, 124, 9648.
- (23) Buckingham, A. D. *Adv. J. Chem. Phys.* **1967**, 12, 107.
- (24) Li, J. B.; Zhang, Q. E. *Sci. China, Ser. B* **1992**, 2, 122 (in Chinese).
- (25) Nakano, M.; Kiribayashi, S.; Yamada, S.; Shigemoto, I.; Yamaguchi, K. *Chem. Phys. Lett.* **1996**, 262, 66.
- (26) Yamada, S.; Nakano, M.; Yamaguchi, K. *J. Phys. Chem. A* **1999**, 103, 7105.